ELSEVIER

Journal of Chromatography A, 911 (2001) 63–73

JOURNAL OF CHROMATOGRAPHY A

www.elsevier.com/locate/chroma

Studies on the response mechanism of thermionic detection to organophosphorus compounds

U.V.R. Vijaya Saradhi[a], M.V.S. Suryanarayana[a,*], A.K. Gupta[a], R.P. Semwal[a], B. Jayaram[b]

[a]*Defence Research and Development Establishment, Jhansi Road, Gwalior 474002, Madhya Pradesh, India*

[b]*Department of Chemistry, Indian Institute of Technology, Hauz Khas, New Delhi, India*

Received 19 July 2000; received in revised form 21 November 2000; accepted 24 November 2000

Abstract

The response of thermionic/nitrogen–phosphorus detection (TID) to a series of organophosphonate esters has been studied. The response of TID is found to decrease with the increase in the alkyl chain length of the molecules. An attempt has been made to propose the response mechanism of TID for these compounds. The charge carriers accountable for the response do not necessarily arise by combustion of the molecule but by a reaction involving alkali metal and the compound. This has been supported by thermodynamic parameters and molecular descriptors. The mechanism of the reaction that appears to be bimolecular has been explained by steric effects. The study successfully explains the observed change in the response of TID with minor changes in structures of the molecules.

Keywords: Thermionic detection; Detection, GC; Organophosphorus compounds

1. Introduction

Thermionic/nitrogen–phosphorus detection (TID) and flame photometric detection (FPD) are two widely used element specific detection methods for the detection of organophosphorus compounds in complex environmental matrices. Modern thermionic/nitrogen–phosphorus detection (NPD) [2], is an improvised version of alkali flame ionization detection (AFID) which was first introduced by Karmen and Guiffrida [1] in 1964. The detector response arises from the interaction of gaseous analyte species with the excited hot alkali ceramic bead, the heart of this detector, which leads to the formation of charge carriers.

The response of such detectors is element specific and explained by the reaction of alkali, its electron, with various phosphorus oxides resulting from the combustion of phosphorus compounds in the flame [1–4] as described by the following equations:

$$P{=}O\rangle + e \rightarrow [\langle P{=}O\rangle]^- \quad (1)$$

$$\langle O{=}P{=}O\rangle + e \rightarrow [\langle {=}P{-}O] \leftrightarrow [O{-}P{=}O\rangle]^- \quad (2)$$

The response should therefore be independent of the molecular configuration. Although, minor differences in the molecular structures can sometimes influence the response as has been observed in case of nitrogen response by Kolb and Bischoff [2], the same has never been investigated with organophos-

*Corresponding author. Tel.: +91-751-341-980; fax: +91-751-341-148.

E-mail address: viro@drde.8m.com (M.V.S. Suryanarayana).

0021-9673/01/$ – see front matter
PII: S0021-9673(00)01190-0

phorus compounds. The investigation described here was initiated to explain the mechanism of TID using the differences in response of the detector among a series of organophosphorus compounds.

Physico–chemical parameters explain the physical and chemical stability of the molecules in gaseous as well as in liquid states. The analytes will generally be in the gaseous state in the gas chromatographic detectors and thermodynamic parameters can successfully explain the stability of the molecules in the gaseous state. The gaseous state reactions depend mainly on the enthalpy of vaporization and Gibbs' free energy functions of the molecules. Also the primary information regarding the cleavage of bonds during a reaction in the molecules is best explained by the molecular descriptors like bond length, bond order, charge densities on the atoms and the force constants of the bonds. Thus the chemical reactions in the gaseous phase of the molecules can be predicted by considering these parameters.

In the present investigation, an attempt has been made to probe into the mechanism of TID with respect to a series of organophosphonate esters and explain the mechanism with respect to the molecular descriptor data and the calculated physico–chemical (thermodynamic) parameters, and steric parameters.

2. Methods

The studies were carried out with four series of organophosphonate esters with gradual increase in the alkyl group chain length. The molecular descriptors and thermodynamic parameters for all the compounds were computed. The molecular descriptors include, the bond lengths, the charge densities on the atoms and the force constant of the bonds. The thermodynamic parameters include, the boiling point, vapor pressure, enthalpy of vaporization and Gibbs free energy of the molecules.

Molecular descriptors namely bond lengths, and charge densities on the atoms were computed by Hyperchem version 5.0 [5]. The structures were built in the builder module of the Hyperchem software, and minimized using the Mm+ force field with bond dipoles as the electrostatic interactions without any cut-offs and Polak–Ribiere conjugate gradient method with RMS gradient 0.1 kcal/[A^0 mol] for a maximum of 500 cycles. The atomic charges in a molecule (considered neutral for this purpose with spin multiplicity 1) were calculated by the EHT method. The unweighted Huckel constant was chosen as 1.75. Tables 3 and 4 present the bond distances obtained from the program itself and the Mm^+ force field energies of the molecules, respectively.

As the force constant of the bond is proportional to the dissociation energy of that bond, the force constant of the P–O–R group was determined by simultaneous gas chromatography–Fourier transform infrared spectrometry (GC–FT-IR) studies in the gaseous phase. GC–FT-IR studies on organophosphorus compounds indicate that the frequency of absorption for the O–C bond lies in the region of 1050–950 cm^{-1} [6]. The significant change in frequency reported to occur only with O–C bond that has a characteristic absorption peak of maximum intensity. The force constants of the O–C bond were calculated using the formula [6,7]:

$$\gamma = \frac{1}{2\pi c} \cdot \sqrt{(k/\mu)} \tag{3}$$

where γ = wave number, k = force constant, c = velocity of light and μ = reduced mass of the atoms in that specific bond.

The GC–FT-IR studies using a light pipe provide the spectra of the molecules in their gaseous phase where liquid phase interactions are absent. The studies of gas phase spectra of the compounds help to decipher the mechanism of TID in which the compounds undergo gas phase ionization on the alkali ceramic bead.

The boiling points of all the compounds at atmospheric pressure were calculated by the GC method with a slight change in the formula:

$$BP_c = BP_n + (BP_{n+1} - BP_n) \cdot \frac{(t_{Rc} - t_{Rn})}{(t_{Rn+1} - t_{Rn})} \tag{4}$$

where BP_c is the boiling point of the compound, t_{Rc} is its retention time, BP_n and BP_{n+1} are the boiling points of the *n*-paraffins eluted, respectively, just before and just after the compound, and t_{Rn} and t_{Rn+1} are the retention times of the two respective *n*-paraffins [8].

The enthalpy of vaporization of the compounds

Table 1
GC–TID response data

No	Name of compound	Structure	Code	Molecular mass	Response factor ($\times 10^9$ mol^{-1})
1.	Dimethyl methyl phosphonate	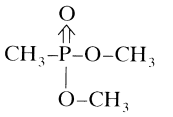	DMMP	124	33.87
2.	Diethyl methyl phosphonate	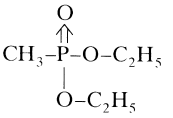	DEMP	152	32.41
3.	Dipropyl methyl phosphonate	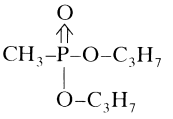	DPMP	180	30.98
4.	Diisopropyl methyl phosphonate	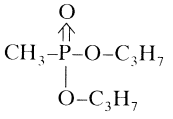	DIMP	180	30.40
5.	Dibutyl methyl phosphonate	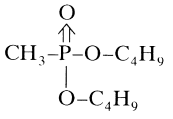	DBMP	208	29.17
6.	Di-sec-butyl methyl phosphonate	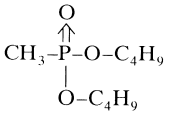	DSBMP	208	28.85
7.	Diisobutyl methyl phosphonate	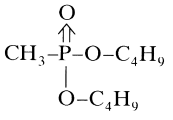	DIBMP	208	28.55
8.	Dimethyl ethyl phosphonate	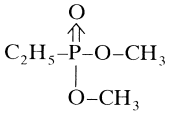	DMEP	138	33.08
9.	Diethyl ethyl phosphonate	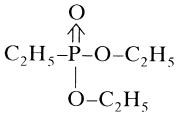	DEEP	166	31.56
10.	Dipropyl ethyl phosphonate	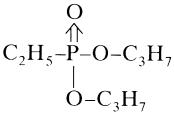	DPEP	194	29.85

Table 1. Continued

No	Name of compound	Structure	Code	Molecular mass	Response factor ($\times 10^9$ mol^{-1})
11.	Diisopropyl ethyl phosphonate	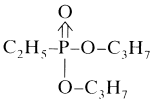	DIPEP	194	29.27
12.	Dibutyl ethyl phosphonate	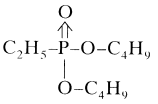	DBEP	222	27.96
13.	Di-sec-butyl ethyl phosphonate	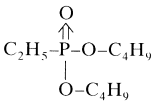	DSBEP	222	27.18
14.	Diisobutyl ethyl phosphonate	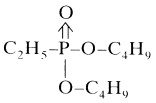	DIBEP	222	27.40
15.	Dimethyl isopropyl phosphonate	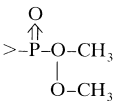	DMIPP	152	32.20
16.	Diethyl isopropyl phosphonate	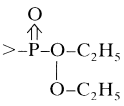	DEIPP	180	30.16
17.	Dipropyl isopropyl phosphonate	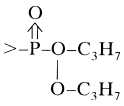	DPIPP	208	28.20
18.	Disopropyl isopropyl phosphonate	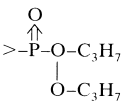	DIPIPP	208	27.58
19	Dibutyl isopropyl phosphonate	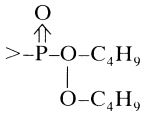	DBIPP	236	25.92

Table 1. Continued

No	Name of compound	Structure	Code	Molecular mass	Response factor ($\times 10^9$ mol^{-1})
20.	Di-sec-butyl isopropyl phosphonate	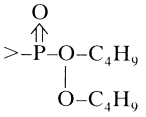	DSBIPP	236	25.10
21.	Diisobutyl isopropyl phosphonate	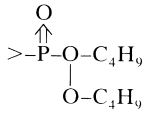	DIBIPP	236	25.45
22.	Dimethyl phosphite	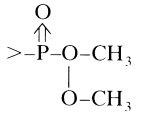	DMP	110	34.46
23.	Diethyl phosphite	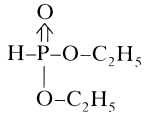	DEP	138	32.65
24.	Dipropyl phosphite	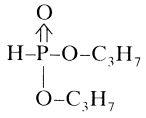	DPP	166	31.32
25.	Diisopropyl phosphite	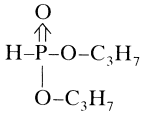	DIPP	166	30.98
26.	Dibutyl phosphite	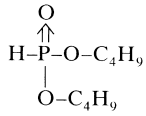	DBP	194	29.60
27.	Di-sec-butyl phosphite	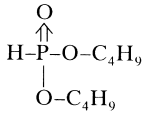	DSBP	194	29.26
28.	Diisobutyl phosphite	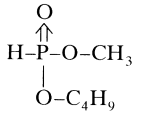	DIBP	194	29.44

was calculated by Troutan's rule that states the change in entropy of vaporization of the liquid is equal to the ratio of enthalpy of vaporization to its boiling point and is constant (~ 85 J/mol) for most of the liquids [9]:

$$\Delta S = \frac{\Delta H}{T_B} = 85 \text{ J/mol} \quad (5)$$

The Gibbs energy is calculated by the formula suggested by Heberger and Kowalska [10]:

$$\Delta\mu_p = \Delta H_v \cdot (T/T_B + 1) \quad (6)$$

The molar responses are calculated by the formula:

$$\text{Response factor} = \frac{\text{Peak area} \cdot \text{molecular mass}}{(\text{volume of injection}) \cdot (\text{amount of sample}) \cdot (\%\ \text{purity})} \quad (7)$$

and are listed in Table 1.

3. Chemicals

All the compounds used in this study except dimethyl methyl phosphonate (DMMP), dimethyl phosphite (DMP), diethyl phosphite (DEP) and diisopropyl phosphite (DIP) were synthesized in the laboratory with the purities above 95% (GC–FID). All these chemicals were characterized by GC, nuclear magnetic resonance (NMR), IR and mass spectral methods. The specified chemicals other than those synthesized were of Aldrich grade. E.-Merck HPLC-grade chemicals, methanol for GC and GC–MS analyses and dichloromethane for the GC–FT-IR studies were used as solvents.

4. Experimental

4.1. Gas chromatography

A CHEMITO 8610 HR gas chromatograph (Mumbai, India) equipped with a DANI thermionic detector and a Hewlett-Packard GC 6890 system with a mass-selective detector (MSD-5973) (USA) were used to compute the response factors and the boiling points and vapor pressures of the compounds, respectively. The test method included a 30 m×0.32 mm I.D., 0.25 μm thickness BP-5 capillary column, and a single-step oven temperature program from 50 to 280°C. The initial and final column temperature hold times were 2 and 5 min, respectively. Oven temperature ramp was 10°C/min. A similar oven temperature program was used for the gas chromatographs in GC–MS and GC–FT-IR. Helium (99.9999%) was used as carrier gas at a flow-rate of 1.2 ml/min whereas hydrogen at 5 ml/min and air at 80 ml/min were used as detector gases. Concentrations of all the solutions were kept constant and a constant volume (0.5 μl) was injected with a Hamilton 10-μl syringe.

4.2. GC–FT-IR

A Perkin-Elmer Model 1720 X GC–FT-IR (USA) was used to record data in the vapor phase of the compounds. The test method included a 25 m×0.53 mm I.D., 1.0 μm thickness BP-5 wide bore capillary column. Nitrogen (99.99%) as carrier gas at 20 p.s.i. was used (1 p.s.i.=6894.76 Pa). The FT-IR resolution was 8 cm^{-1} and the number of scans per second was 16. The IR interface was less than 204 light pipes and the transfer line temperature was 280°C. The FT-IR's MCT detector was kept at liquid nitrogen temperature.

5. Results and discussion

Most TID systems can be operated in two modes: in an element specific phosphorus mode where P containing compounds only are detected and in another mode where both P and N containing compounds are traced [11]. The difference of these two working modes is mainly due to the operating conditions of the hydrogen flame, oxidizing flame for P compounds and a reducing flame for both P and N compounds. In our present experimental set-up, the detector was used in the N/P mode, which omits a flame in the traditional way. The alkali bead is heated electrically and a small hydrogen flow (5 ml/min) forms a plasma around the ceramic bead. Thus, a reducing atmosphere is created rather than an oxidizing flame, ruling out the possibility of formation of phosphorus oxides. Under these conditions, the original molecule comes in contact with alkali and/or the electron immediately. This makes it possible that minor differences in the molecular structure may influence the response as shown by the experimental data (Table 1).

Table 1 depicts the TID response data of the organophosphorus compounds studied. It is evident from the data that the dialkyl phosphites give higher responses followed by methyl, ethyl and isopropyl

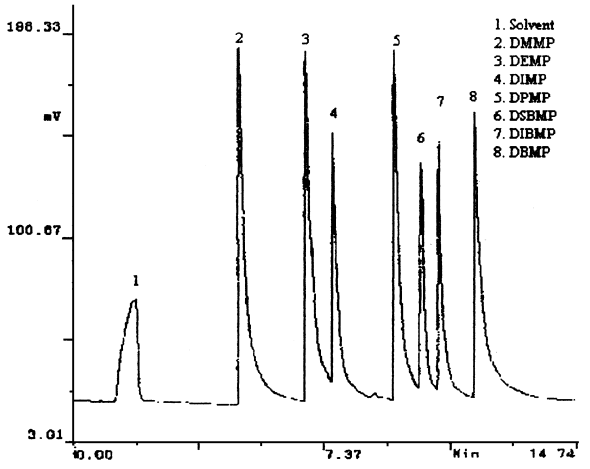

Fig. 1. GC–TID chromatogram of an equimolar mixture of the methyl phosphonate series.

phosphonate series. TID response is lowered with the alkyl chain increments in the molecules. This is true in either case where the alkyl group is connected to an oxygen atom (in P–O–R ester bond) or to phosphorus atom (P–R bond). Also, lower response was observed for the branched chain compounds than the corresponding normal chain compounds. The trend of response among a series of compounds was shown in Figs. 1 and 2, representing the chromatograms of equimolar mixtures of methyl and isopropyl phosphonate series of compounds, respectively.

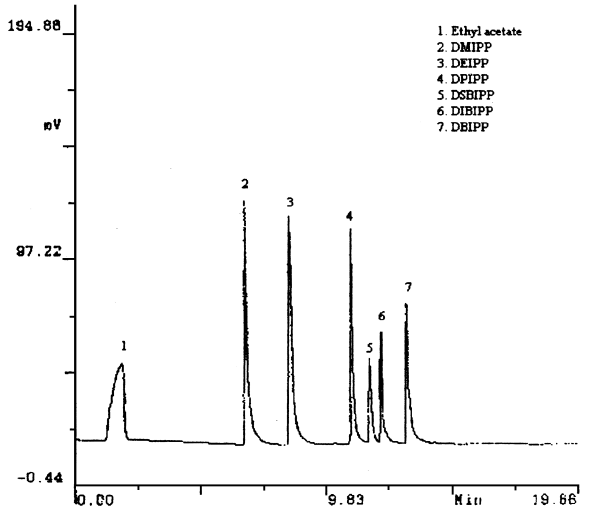

Fig. 2. GC–TID chromatogram of an equimolar mixture of the isopropyl phosphonate series.

If the reaction is combustion, it is governed by the thermodynamic parameters like Gibbs' energy and enthalpy of vaporization, which explain the stability of the molecules in the gaseous state. The ease of combustion of a reactant depends on the Gibbs energy and the enthalpy of the molecules as higher the values of these parameters, higher is the molecular stability and thus, decrease in combustion. This could then be directly correlated with the formation of charge carriers in the detector. From Table 2, it is evident that Gibbs energy increases with increase in the alkyl groups in the molecule. The response factors presented in Table 1 can also be seen to decrease in the same order as the increase in the energy functions except for the branched chain compounds. The branched chain compounds gave a lower response than their corresponding normal chain compounds as the Gibbs energy and enthalpy of the former are lower than the latter. This indicates that the TID reaction may not be exactly the combustion reaction but can be a chemical reaction between the molecule with alkali and/or the electron.

Further, we attempted to probe into the mechanism of the detector considering that the fragmentation of the molecules in the detector as a chemical reaction between the molecule and the excited alkali metal atom. For this, we calculated the molecular descriptors, namely, bond lengths and force constants, and the atomic charge densities in the molecules. With these molecular descriptors, it is possible to find the actual site of bond cleavage in the molecules.

The bond distances computed using the Hyperchem software are shown in Table 3. It is evident from the data, that only the O–C bond distance is being changed with the change in the alkyl group on the oxygen atom present in the P–O–R ester linkage. The bond length is observed to be increasing with increase in the alkyl group and a drastic increase is observed in the case of branched chain alkyl groups. This shows that the alkyl group can easily be knocked out by the incoming nucleophiles. Thus, it shows that the site of cleavage in the molecule is the O–R bond in the P–O–R ester linkage.

The atomic charges on different elements in the

Table 2
Thermodynamic parameters for the compounds investigated

Compound	Boiling point (°C)	Enthalpy of vaporization (kJ/mol)	Gibbs' free energy (kJ/mol)
DMMP	187	39.1	64.43
DEMP	212	41.22	66.55
DPMP	247	44.2	69.53
DIMP	219	41.82	67.15
DBMP	279	46.92	72.25
DSBMP	263.6	45.611	70.94
DIBMP	254	44.79	70.11
DMEP	203.6	40.511	65.84
DEEP	226	42.415	67.745
DPEP	251	44.54	69.87
DIPEP	239	43.52	68.85
DBEP	289.6	47.821	73.15
DSBEP	266.5	45.858	71.19
DIBEP	275	46.58	71.91
DMIPP	209	40.97	66.3
DEIPP	230	42.755	68.085
DPIPP	264.5	45.688	71.02
DIPIPP	237	43.35	68.68
DBIPP	292	48.025	73.35
DSBIPP	270	46.155	71.48
DIBIPP	278	46.835	72.165
DMP	169	37.57	62.9
DEP	200	40.205	65.535
DPP	238	43.435	68.765
DIP	213	41.31	66.64
DBP	273	46.41	71.74
DSBP	249.7	44.43	69.76
DIBP	257	45.05	70.38

molecule computed by Hyperchem software are presented in Table 4. The variations in the atomic charges on the elements with the change in the alkyl groups are negligible and can be omitted from the studies. But significant changes do take place whenever there is an increase in the branching at the first carbon from the oxygen side in the P–O–R bond. An increase in the negative charge on oxygen atom in these cases enhance the $p\pi$–$d\pi$ bond energy and the alkyl group can be knocked out easily as the resulting species is stable in a resonating form.

The results of GC–FT-IR data in Table 5 show that the force of attraction between the oxygen and carbon atoms in the compounds studied generally decrease with the increase in the alkyl chain length as well as branching. This may be due to the increase in +I effect by the increased chain length in P–O–C bond, where the electron pair on the oxygen atom can easily be donated to the phosphorus atom. This increases the $p\pi$–$d\pi$ bonding efficiency in the molecule, the electron cloud on the oxygen atom gets shifted towards the phosphorus atom, thus decreasing the reactivity of the phosphorus atom. In addition, due to the shift in the electron cloud, the force of attraction between the alkyl group and the oxygen atom decreases, thus weakening the bond.

The excited alkali metal atom could attack the central phosphorus atom which can accommodate the electrons because of the presence of vacant d-orbitals. As the alkali atom approaches the phosphorus atom, the alkyl group attached to the oxygen atom leaves the molecule as alkyl radical following a homolytic fission of the O–C bond. Here the reaction may proceed in two ways. The first one is the formation of the phosphonyl radical which further reacts with another alkali atom to form a negatively charged species as shown in Scheme 1. The second possibility is that the ion formation can occur by the

Table 3
Bond lengths of some specific bonds in the molecule

Compound	P–O	P–C	O–C	P=O
DMMP	1.68914	1.79228	1.40736	1.60445
DEMP	1.68909	1.7922	1.41008	1.60458
DPMP	1.68878	1.79172	1.40984	1.6043
DIMP	1.68835	1.79124	1.4142	1.60235
DBMP	1.68939	1.79159	1.41048	1.60384
DSBMP	1.68918	1.79351	1.4168	1.6007
DIBMP	1.68883	1.79237	1.41143	1.60156
DMEP	1.68873	1.79608	1.40469	1.60818
DEEP	1.68856	1.79607	1.40279	1.60839
DPEP	1.68876	1.79579	1.40765	1.6085
DIPEP	1.68786	1.79863	1.41423	1.60011
DBEP	1.68845	1.79633	1.40739	1.6082
DSBEP	1.69144	1.79863	1.41326	1.60013
DIBEP	1.68789	1.79713	1.41095	1.6019
DMIPP	1.69279	1.80195	1.4088	1.6022
DEIPP	1.69234	1.80219	1.41217	1.6007
DPIPP	1.69313	1.80241	1.4122	1.60033
DIPIPP	1.69036	1.80524	1.41374	1.59941
DBIPP	1.68969	1.80206	1.4123	1.60287
DSBIPP	1.68914	1.80283	1.41532	1.60234
DIBIPP	1.68886	1.80132	1.41077	1.60195
DMP	1.72583	1.38061	1.40752	1.61794
DEP	1.72593	1.38075	1.41027	1.61803
DPP	1.72618	1.38075	1.41029	1.61804
DIP	1.72385	1.38002	1.41527	1.61732
DBP	1.72616	1.38055	1.41035	1.61837
DSBP	1.72179	1.37952	1.41646	1.6155
DIBP	1.72439	1.38072	1.41036	1.61733

supply of an electron from the alkali metal atom with simultaneous cleavage of alkali radical as shown in Scheme 2. The approach of the alkali atom towards the central phosphorus atom is governed by the steric effects of the adjacent groups present in the molecule. The steric effects are generally more pronounced whenever there is branching in the molecule. The reaction thus becomes slow with increase in the branching. This may be the reason why the branched chain compounds gave lower response than their corresponding normal chain compounds.

To confirm the steric effects of the molecules, we performed positive chemical ionization (PCI) for all the compounds (data shown in Table 6) with methane. In PCI with methane, the organophosphorus compounds generally give $(M+H)^+$, $(M+29)^+$ and $(M+41)^+$. If the steric effects in the molecule predominate, then the next two peaks

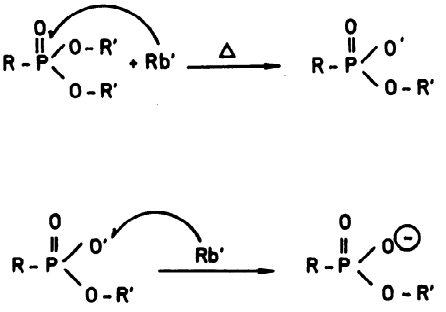

Scheme 1.

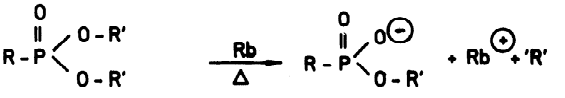

Scheme 2.

should be absent in case of highly sterically hindered molecules. All the compounds show all the three ions except diisopropyl, di-sec-butyl and diisobutyl compounds. The first two did not show $(M+29)^+$ and $(M+41)^+$ and the latter did not show only $(M+29)^+$. From this, it is clear that the steric effects regulate the formation of the addition products indirectly indicating that the TID response mechanism is also governed by steric factors.

The positively charged alkali ions will be collected by the alkali ceramic bead in the detector which is generally biased to a negative potential. The reaction appears to proceed through a bimolecular path way as the response is increased both with increase in concentration of the solute and the electric current supplied to the ceramic bead which increases the alkali metal concentration in the detector.

6. Conclusion

The response of TID to organophosphorus compounds changes significantly with small structural changes of the molecules when it is used in the conditions that are necessary for the detection of both nitrogen and phosphorus compounds. The response decreases with increase in the bulkiness of the alkyl groups in the molecules. The process of

Table 4
Charges on different atoms in the molecules

Compound	Charge				
	P	O of P=O	O of P–O	C of O–C	C of P–C
DMMP	2.310	−1.444	−0.880	0.422	−0.143
DEMP	2.311	−1.446	−0.890	0.475	−0.143
DPMP	2.311	−1.445	−0.893	0.468	−0.143
DIMP	2.313	−1.436	−0.909	0.530	−0.143
DBMP	2.312	−1.444	−0.895	0.466	−0.143
DSBMP	2.314	−1.431	−0.912	0.527	−0.150
DIBMP	2.316	−1.432	−0.905	0.468	−0.147
DMEP	2.303	−1.460	−0.879	0.423	−0.065
DEEP	2.304	−1.460	−0.890	0.477	−0.065
DPEP	2.304	−1.461	−0.892	0.469	−0.065
DIPEP	2.315	−1.428	−0.913	0.531	−0.091
DBEP	2.304	−1.460	−0.892	0.467	−0.065
DSBEP	2.314	−1.428	−0.915	0.523	−0.090
DIBEP	2.316	−1.435	−0.901	0.467	−0.084
DMIPP	2.313	−1.436	−0.894	0.424	−0.024
DEIPP	2.317	−1.430	−0.913	0.484	−0.028
DPIPP	2.317	−1.429	−0.916	0.476	−0.027
DIPIPP	2.312	−1.426	−0.904	0.530	−0.038
DBIPP	2.316	−1.439	−0.908	0.473	−0.025
DSBIPP	2.314	−1.438	−0.914	0.527	−0.029
DIBIPP	2.317	−1.437	−0.909	0.469	−0.026
DMP	2.213	−1.419	−0.868	0.425	0.040
DEP	2.214	−1.420	−0.879	0.479	0.041
DPP	2.214	−1.420	−0.881	0.472	0.041
DIP	2.216	−1.412	−0.892	0.532	0.040
DBP	2.214	−1.420	−0.881	0.469	0.041
DSBP	2.215	−1.412	−0.895	0.524	0.036
DIBP	2.217	−1.415	−0.886	0.470	0.039

Table 5
GC–FT-IR data

Compound	Wave number in IR spectrum (cm^{-1})	Force constant value ($\cdot 10^5$ dyne cm)
DMMP	1051	4.461
DEMP	1045	4.410
DPMP	1003	4.063
DIMP	994	3.990
DBMP	1029	4.276
DMEP	1051	4.461
DEEP	1046	4.419
DPEP	1050	4.453
DIPEP	1010	4.120
DBEP	1027	4.260
DSBEP	984	3.910
DIBEP	994	3.990
DMIPP	1046	4.419
DEIPP	1038	4.351
DPIPP	1000	4.039
DIPIPP	990	3.981
DBIPP	1027	4.260
DSBIPP	994	3.990
DIBIPP	1018	4.186
DMP	989	3.950
DEP	986	3.926
DIP	979	3.871
DBP	980	3.879
DSBP	976	3.847

Table 6
PCI mass spectral data

Compound	PCI mass spectral data[a]
DMMP	123, 153, 165
DEMP	153, 181, 193, 125, 97
DPMP	181, 139, 97, 209, 221, 167
DIMP	181, 97, 139, 125, 167
DBMP	209, 153, 97, 237, 249, 181, 125, 137
DSBMP	209, 97, 153, 125
DIBMP	209, 153, 97, 125, 181, 249
DMEP	139, 167, 179
DEEP	166, 195, 207, 139
DPEP	195, 223, 235
DIPEP	195, 223, 235
DBEP	223, 111, 139, 167, 151, 249, 263
DSBEP	223, 111, 139, 167
DIBEP	223, 111, 167, 139, 195, 263
DMIPP	153, 110, 167, 193, 79, 95
DEIPP	181, 221, 138, 65, 125, 82, 111, 93
DPIPP	209, 125, 167, 149, 65, 83, 107, 249
DIPIPP	209, 125, 167, 153, 195
DBIPP	237, 125, 181, 209, 153, 166, 222, 265, 277
DSBIPP	237, 125, 181, 153, 209
DIBIPP	237, 181, 125, 153, 209, 277

[a] Mass spectral data are presented in the decreasing order of their intensities.

ionization in the detector may not be because of combustion, but may be due to the reaction of the alkali metal atom/electron with the compounds. Thermodynamic parameters and molecular descriptors presented here support this argument and the ionization is governed by the molecular geometry/steric effects in the molecules. Thus, the possible mechanism presented here seems to be reasonable to explain the variation in response for the presented organophosphorus compounds.

References

[1] A. Karmen, L. Guiffrida, Nature 201 (1964) 1204.
[2] B. Kolb, J. Bischoff, J. Chromatogr. Sci. 12 (1974) 625.
[3] D.D. Bombick, J. Allison, J. Chromatogr. Sci. 27 (1989) 612.
[4] P. van de Weijer, B.H. Zwerver, R.J. Lynch, Anal. Chem. 60 (1988) 1380.
[5] Hyperchem Version 5.0, Hypercube, USA.
[6] L.J. Ballamy, The Infra-Red Spectra of Complex Molecules, Chapman and Hall, London, 1975.
[7] K.D. Berlin, G.M. Blackburn, J.S. Cohen, D.E.C. Corbridge, D.M. Hellwege, Topics in Phosphorus Chemistry, Vol. 6, Interscience-Wiley, 1969.
[8] M. Dorbon, S. Lamaison, A. Chevalier, J. Chromatogr. 557 (1991) 155.
[9] P.W. Atkins, Physical Chemistry, 4th ed., Oxford University Press, Oxford, 1990.
[10] K. Heberger, T. Kowalska, Chromatographia 48 (1998) 89.
[11] J. Sevcik, Detectors in Gas Chromatography, Journal of Chromatography Library, Elsevier, Amsterdam, 1975.